JOURNAL OF GEOPHYSICAL RESEARCH, VOL. 98, NO. D10, PAGES 18,471–18,488, OCTOBER 20, 1993

A Physical Retrieval of Cloud Liquid Water Over the Global Oceans Using Special Sensor Microwave/Imager (SSM/I) Observations

THOMAS J. GREENWALD, GRAEME L. STEPHENS, THOMAS H. VONDER HAAR AND DARREN L. JACKSON

Department of Atmospheric Science, Colorado State University, Fort Collins

A method of remotely sensing integrated cloud liquid water over the oceans using spaceborne passive measurements from the special sensor microwave/imager (SSM/I) is described. The technique is comprised of a simple physical model that uses the 19.35- and 37-GHz channels of the SSM/I. The most comprehensive validation to date of cloud liquid water estimated from satellites is presented. This is accomplished through a comparison to independent ground-based microwave radiometer measurements of liquid water on San Nicolas Island, over the North Sea, and on Kwajalein and Saipan Islands in the western Pacific. In areas of marine stratocumulus clouds off the coast of California a further comparison is made to liquid water inferred from advanced very high resolution radiometer (AVHRR) visible reflectance measurements. The results are also compared qualitatively with near-coincident satellite imagery and with other existing microwave methods in selected regions. These comparisons indicate that the liquid water amounts derived from the simple scheme are consistent with the ground-based measurements for nonprecipitating cloud systems in the subtropics and middle to high latitudes. The comparison in the tropics, however, was less conclusive. Nevertheless, the retrieval method appears to have general applicability over most areas of the global oceans. An observational measure of the minimum uncertainty in the retrievals is determined in a limited number of known cloud-free areas, where the liquid water amounts are found to have a low variability of 0.016 kg m^{-2}. A simple sensitivity and error analysis suggests that the liquid water estimates have a theoretical relative error typically ranging from about 25% to near 40% depending on the atmospheric/surface conditions and on the amount of liquid water present in the cloud. For the global oceans as a whole the average cloud liquid water is determined to be about 0.08 kg m^{-2}. The major conclusion of this paper is that reasonably accurate amounts of cloud liquid water can be retrieved from SSM/I observations for nonprecipitating cloud systems, particularly in areas of persistent stratocumulus clouds, with less accurate retrievals in tropical regions.

1. INTRODUCTION

The liquid water content of clouds is one of several components of the atmospheric water budget that has a far-reaching influence on the Earth's radiative energy balance. Because of the strong interactions between cloud water and radiation, clouds may play an important part in global climate through the so-called cloud liquid water feedback, as several studies have proposed [e.g., *Paltridge*, 1980; *Somerville and Remer*, 1984]. Certain aspects of the relationship between liquid water and the Earth radiation budget (ERB) have been investigated recently in the observational study of *Stephens and Greenwald* [1991], where it is demonstrated that the response of the ERB to large-scale changes in cloud liquid water may not be unique over the global oceans and appears to differ significantly in the midlatitudes and tropics. For these reasons it is essential that we understand how cloud liquid water is maintained on a global scale, how it is distributed in space, and how it varies from season to season and year to year.

The estimation of cloud liquid water and other geophysical quantities (e.g., precipitable water, surface winds, precipitation, and others) over the oceans from spaceborne passive microwave instruments has a long history that spans more than two decades. *Basharinov et al.* [1969] and *Akvilonova et al.* [1973] were among the first studies to utilize such measurements to infer information about the water content of the atmosphere. Many other studies followed these pioneering efforts based on observations from different instruments on a variety of satellites including the Nimbus E microwave spectrometer (NEMS) on the Nimbus 5 spacecraft [e.g., *Grody*, 1976; *Chang and Wilheit*, 1979], the scanning microwave spectrometer (SCAMS) aboard the Nimbus 6 satellite [*Grody et al.*, 1980; *Rosenkrantz et al.*, 1978], and the special multichannel microwave radiometer (SMMR) on the Nimbus 7 and Seasat satellites [e.g., *Njoku and Swanson*, 1983; *Prabhakara et al.*, 1983; *Curry et al.*, 1990].

The latest microwave instrument, which is presently aboard the F-8, F-10, and F-11 Defense Meteorological Satellite Project (DMSP) satellites, is the special sensor microwave/imager (SSM/I). The principal data used in this study are the brightness temperatures obtained from the SSM/I on board the DMSP F-8 satellite, which was launched June 19, 1987. The imager consists of seven channels that measure both vertically and horizontally polarized radiation at 19.35, 37, and 85.5 GHz and strictly vertically polarized radiation at 22.235 GHz. For the channels that are of interest to this study, the spatial resolution of the 19.35-GHz channels is 69×43 km and for the 37-GHz channels it is about 37×28 km.

The cloud liquid water retrieval schemes that have been developed thus far for the SSM/I have been, for the most part, statistically based. The purely statistical method of *Alishouse et al.* [1990] and the semistatistical method of *Hargens* [1992] can be applied to the global oceans. Other investigators such as *Petty* [1990] have taken a different path

Paper number 93JD00339.
0148-0227/93/93JD-00339$05.00

and use a semiphysical approach based on a simple physical model to estimate liquid water over specific regions of the ocean. The work of *Jones and Vonder Haar* [1990] involves one of the few attempts that has been made to estimate cloud liquid water over land areas, which consists of a physically based iterative technique that was applied on a case study basis.

The primary goal of this study is to develop and validate a simple physical scheme that can be used to retrieve cloud liquid water from SSM/I observations on a global basis over the ice-free oceans . Our motivation for developing a new retrieval algorithm is that unlike the retrieval of precipitable water for which much research has been done and several different methods are available [e.g., *Schluessel and Emery*, 1990; *Petty*, 1990; *Tjemkes et al.*, 1991], there is a conspicuous lack of rigorously tested global cloud liquid water algorithms available for the SSM/I.

Because of the nearly complete absence of "ground truth" observations, previous investigators dealing with cloud liquid water retrieval have been unable to verify their results. In this study we present a strategy to validate liquid water amounts derived from satellites. This is done through a comparison to coincident observations of integrated liquid water from ground-based microwave radiometers at four different locations over the oceans.

One issue that we believe has not been sufficiently addressed in the literature concerns the errors associated with cloud liquid water retrieval over the oceans from space. A more thorough treatment of these errors is warranted since measurements of liquid water may be potentially useful, for example, in global climate studies [*Stephens and Greenwald*, 1991] and in the analysis of weather systems [e.g., *Rosenkranz et al.*, 1978; *Katsaros and Lewis*, 1986]. Here an attempt is made to determine quantitative theoretical estimates of the retrieval error under a variety of atmospheric and sea surface conditions.

In the first part of this paper we develop a simple physical model that is used to simultaneously estimate integrated water vapor and cloud liquid water. A discussion of the calibration of the model is presented in section 3. Section 4 involves the validation of the liquid water amounts derived from the present model through a comparison to coincident ground microwave radiometer measurements and to near-coincident liquid water derived from the advanced very high resolution radiometer (AVHRR) for stratocumulus clouds off the coast of California. The validation is followed in section 5 by a sensitivity and error analysis of the derived liquid water for areas outside of precipitation under different atmospheric and surface conditions. Global fields of cloud liquid water derived from the present method are shown in section 6 and are compared to previous results from the SMMR and to total cloudiness obtained from the International Satellite Cloud Climatology Project (ISCCP). Finally, the conclusions drawn from this study are presented in section 7.

2. PHYSICAL RETRIEVAL METHOD

In the development of the physical model we begin with the precipitable water content (PWC) retrieval method of *Tjemkes et al.* [1991], which uses 19.35-GHz measurements from the SSM/I. It is shown here in a slightly different form as

$$W = -\frac{\mu}{2\kappa_{w19}} \ln\left[\frac{\Delta T_{19}}{T_s r_{19v}(1-F_{19})\mathcal{T}_{ox19}^2}\right], \qquad (1)$$

where μ is the cosine of the incidence angle, $\mathcal{T}_{ox19}$ is the oxygen transmittance at 19.35 GHz, T_s is the sea surface temperature (SST), $\Delta T_{19} \equiv T_{19h} - T_{19v}$, κ_{w19} is the water vapor mass absorption coefficient and slightly modified from the study of Tjemkes et al. to be 2.58×10^{-3} kg^{-1} m$^2(300/T_s)^{0.477}$, r_{19v} is the sea surface reflectivity at vertical polarization, which is to an excellent approximation $1 - \epsilon_{19v}$, and [e.g., *Wilheit*, 1979]:

$$F_{19} = \frac{T_{19h} - \overline{T}}{T_{19v} - \overline{T}} \approx \frac{r_{19h}}{r_{19v}}, \qquad (2)$$

where

$$\overline{T} = T_s + \Gamma H_w(1 - \mathcal{T}_{w19})\mathcal{T}_{ox19}, \qquad (3)$$

Γ is the temperature lapse rate, and H_w is the water vapor scale height. The second term on the right-hand side of (3) is to account for the dependence of the effective emission height of water vapor on W (see *Tjemkes et al.* [1991] for details).

To simplify the retrieval of PWC, Tjemkes et al. assumed $\overline{T} \approx T_s$. The approximation in (2) works well under this assumption for a relatively transparent atmosphere but breaks down for PWC greater than about 20–25 kg m^{-2}. This conclusion is based on theoretical calculations and a comparison of PWC retrievals with radiosonde observations under mostly clear sky conditions. For retrievals of PWC > 25 kgm^{-2}, the full expression for $\overline{T}$ is used but is in a slightly different form than (3) and is expressed as

$$\overline{T} = T_s + \Gamma H_w(1 - f\mathcal{T}_{w19}^2)\mathcal{T}_{ox19}, \qquad (4)$$

where Γ and H_w are set to typical values of –5.8 K km^{-1} and 2.2 km, respectively, and $f = \exp(50\kappa_{w19}/\mu)$. The empirical factor, f, is to prevent a discontinuity in the retrievals near 25 kg m^{-2}.

As a result of the changes that have been made to the *Tjemkes et al.* [1991] PWC algorithm, it is appropriate to show a comparison of the water vapor amounts derived from the present method (equation (7)) to near-coincident radiosonde measurements. The validation is somewhat limited and involves radiosonde measurements of PWC over the North Sea during the International Cirrus Experiment (ICE) in 1989 and in the West Pacific during the 1990 Tropical Cyclone Motion (TCM) Experiment. The ICE measurements were taken on the R/V *Poseidon* and consist of 29 cases. These measurements were all within 2 hours of a DMSP overpass and frequently were within half an hour to several minutes. In order to have an adequate sample of radiosonde measurements from the TCM Experiment the criterion was increased to ±3 hours within a satellite overpass, which resulted in a total of 292 observations. These observations originated from both small island stations and ships scattered throughout the West Pacific. Cases where precipitation may have been occurring were eliminated and only SSM/I pixels inside of a 50-km radius of the site were used. The results of the comparison, which are shown in Figure 1, are good for a wide range of water vapor values, where the rms difference is 1.9 kg m^{-2} for the ICE measurements and 5.9 kg m^{-2} for the TCM measurements.

It is evident from (1) that the obvious effects introduced by clouds are neglected. This is a reasonable assumption for optically thin clouds, which do not significantly alter the 19.35-GHz brightness temperature. However, as pointed out by Tjemkes et al., a cloud possessing a moderate water content of 0.25 kg m^{-2}, which is typical of thick marine stratocumulus clouds, can cause an error in the instantaneous

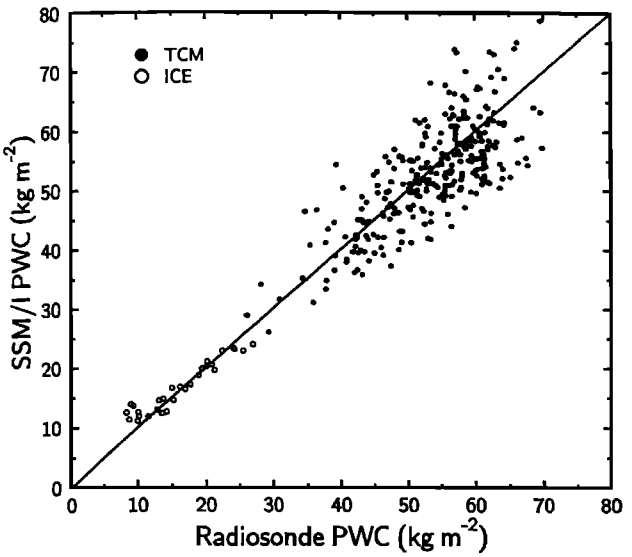

Fig. 1. Comparison of special sensor microwave/imager (SSM/I)-derived precipitable water (kg m^{-2}) and radiosonde measurements during the 1989 International Cirrus Experiment (ICE) and the 1990 Tropical Cyclone Motion (TCM) Experiment.

retrieval of PWC of roughly 5 kg m^{-2}. If we include the transmittance of a nonprecipitating cloud in (1) and assume $\mathcal{T}_{w19} = \exp(-\kappa_{w19}W/\mu)$ and $\mathcal{T}_{\ell 19} = \exp(-\kappa_{\ell 19}L/\mu)$, we can write

$$\kappa_{w19}W + \kappa_{\ell 19}L = -\frac{\mu}{2}\ln\left[\frac{\Delta T_{19}}{T_s r_{19v}(1-F_{19})\mathcal{T}_{ox19}^2}\right], \quad (5)$$

where $\kappa_{\ell 19}$ is the liquid water mass aborption coefficient and L is the vertically integrated liquid water content or liquid water path (LWP) of the cloud.

The other frequency used in the retrieval method is 37 GHz, which lies in a window region and is more responsive to cloud liquid water than 19.35 GHz. We may write an expression analogous to (5) for the 37-GHz channels as

$$\kappa_{w37}W + \kappa_{\ell 37}L = -\frac{\mu}{2}\ln\left[\frac{\Delta T_{37}}{T_s r_{37v}(1-F_{37})\mathcal{T}_{ox37}^2}\right], \quad (6)$$

where $\Delta T_{37} \equiv T_{37h} - T_{37v}$, $r_{37v} = 1 - \epsilon_{37v}$, and $F_{37} = (T_{37h} - T_s)/(T_{37v} - T_s)$. Thus (5) and (6) constitute a set of linear equations that has the following solutions:

$$W = \frac{\tau_1\kappa_{\ell 37} - \tau_2\kappa_{\ell 19}}{\delta} \quad (7)$$

$$L = \frac{\tau_2\kappa_{w19} - \tau_1\kappa_{w37}}{\delta} \quad (8)$$

where

$$\delta = \kappa_{w19}\kappa_{\ell 37} - \kappa_{w37}\kappa_{\ell 19}$$

and τ_1 and τ_2 are the right-hand sides of (5) and (6) respectively, which in physical terms represent the optical depths of the total atmospheric water (outside regions of precipitation and excluding ice) at both frequencies. The procedure for finding W and L is to first apply (7) and (8) using $F_{19} = (T_{19h} - T_s)/(T_{19v} - T_s)$. If $W \leq 25$ kg m^{-2}, then no further calculations are necessary. On the other hand, if $W > 25$ kg m^{-2} the retrieved values are used as initial guesses in deriving iterative solutions, where F_{19} is a function of W as shown in (2) and (4).

A number of models exist [e.g., *Wilheit*, 1979; *Petty*, 1990] that may be used to compute the sea surface emissivities in (5) and (6). For the purposes of this study the emissivity model of *Petty* [1990] is used since it has been carefully calibrated against SSM/I observations. The near-surface wind speed, which is required as input to the model, is retrieved from SSM/I measurements using the global statistical method of *Goodberlet et al.* [1989]. A recent study by *Bates* [1991] suggests that the Goodberlet et al. algorithm may have problems in regions of high SST and PWC, such as in the western tropical Pacific. Therefore in this study the Bates algorithm is used in regions that generally have large amounts of water vapor, which we have arbitarily defined for monthly mean SSTs that reach beyond 300 K. The SST data that are used are those produced operationally by the National Meteorological Center, which are on a 2° × 2° global grid and consist of ship and buoy observations that are blended with satellite data [*Reynolds*, 1988].

The oxygen transmittance at 19.35 and 37 GHz ($\mathcal{T}_{ox19}$ and $\mathcal{T}_{ox37}$) were determined using the transmission model of *Liebe* [1985] and 81 radiosonde profiles over the ocean. Figure 2 shows the oxygen transmittance at 19.35 and 37 GHz versus surface air temperature, which is used here as a surrogate for the temperature profile. It can be seen from this figure that the transmission increases at both frequencies as the lower to middle tropospheric temperatures rise. To account for this apparent temperature effect, an equation of the form $\mathcal{T}_{ox} = a + bT_s + cT_s^2 + dT_s^3$ is fit through the points, where T_s is the monthly mean SST in degrees Celsius. The best fit coefficients are shown in Table 1.

One of the most difficult parameters in the model to estimate is the cloud temperature T_c. *Pandey et al.* [1983] have shown that it is certainly possible (albeit in a highly statistical way) to infer cloud temperature from multichannel microwave measurements along with cloud top temperature information from infrared (IR) observations. A much simpler approach is used in this study to specify the cloud temperature. Since we have no a priori knowledge of the height and temperature of the cloud base or the cloud thickness, a climatological effective cloud temperature is estimated based on monthly mean SSTs. The justification is that the temperature of the cloud, in a climatological sense, roughly follows the sea surface temperature. Thus we let $T_c \approx T_s - 6$ K, which is considered to be representative of most marine boundary layer clouds. A limitation of this crude approximation is that if the cloud is near the sea surface or if a temperature inversion is present, which often occurs at high latitudes, then the retrieved liquid water may be underestimated. For high clouds or clouds with large vertical extent an overestimation in the retrieval of liquid water will likely result.

The liquid water mass absorption coefficients, $\kappa_{\ell 19}$ and $\kappa_{\ell 37}$, are functions of the cloud temperature and are computed from the formulas of *Petty* [1990]. The cubic fit coefficients are shown in Table 1 and apply to temperatures in units of degrees Celsius. In the calculation of these absorption coefficients it is assumed, for simplicity, that the effective temperature of the cloud is the same at 19.35 and 37 GHz. This may not be strictly true since the weighting functions for these two frequencies peak at slightly different levels and hence different temperatures.

It is important to note that the model developed in this study is identical in principle to the dual-frequency physical methods first adopted, for example, by *Akvilonova and Kutuza* [1979] and later implemented by *Grody et al.* [1980]. Therefore the present method is a refinement of these pre-

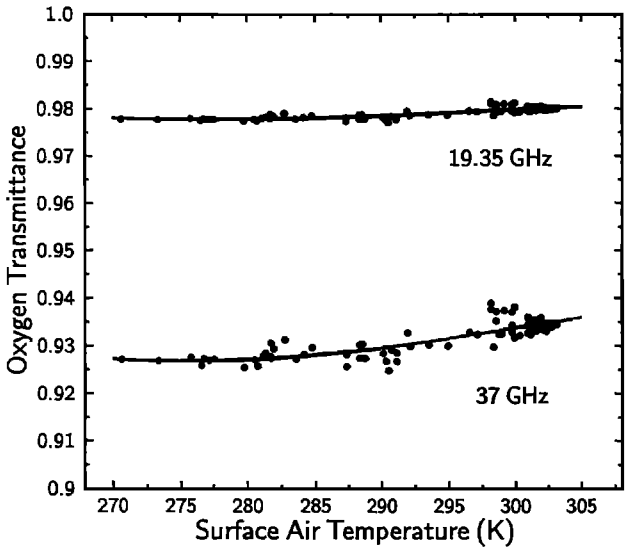

Fig. 2. Theoretical calculations of oxygen transmission at 19.35 and 37 GHz versus surface air temperature (K) for 81 rawinsonde temperature profiles over the ocean. Also indicated are cubic fits to the data points for each frequency, whose coefficients are shown in Table 1.

vious techniques. The study of Grody et al., which is confined to the tropical and subtropical Pacific, differs from the present method in that the cloud and sea surface properties are held fixed. Another distinction of the present method from this earlier work includes a procedure to calibrate the model.

In regions of precipitating cloud systems the retrieval of cloud liquid water and PWC becomes especially difficult because of the dominant influence of absorption and scattering of microwave radiation by precipitation size particles. The upwelling radiation at 19.35 GHz over these cloud systems consists mainly of the strong emission by raindrops below the freezing level [*Spencer et al.*, 1989], while at 37 GHz both absorption and volume scattering effects by raindrops are important. Precipitation in the solid phase has little effect at these frequencies since the absorption by ice is negligible. However, in the presence of large ice particles, radiation at 37 GHz can be scattered as well as polarized [e.g., *Adler et al.*, 1990].

There are a number of methods, both scattering and attenuation based, that are available to identify SSM/I pixels suspected of being contaminated by precipitation [e.g., *Spencer et al.*, 1989; *Petty*, 1990; *Liu and Curry*, 1992]. Rather than applying these techniques, we have chosen instead to use a cloud liquid water threshold of 0.5 kg m^{-2} to detect situations where there might be substantial rainfall within the FOV of the instrument. While this criterion may appear to be arbitrary, it has support from various studies as being, on average, a value associated with the initiation of rain [e.g., *Curry et al.*, 1990; *Liu and Curry*, 1992]. For the purpose of minimizing biases in the monthly mean liquid water, which would probably occur if cloud liquid water was neglected in precipitating cloud systems, the LWP is set to a constant value of 0.5 kg m^{-2} for SSM/I pixels identified as being rain contaminated.

3. Model Calibration

The main purpose of the calibration process is to arrive at an estimate of the one physical quantity that remains to be specified in the model, namely, κ_{w37}, and to account for uncertainties in oxygen and water vapor transmission at 37 GHz, possible biases in the sea surface emissivity model and brightness temperatures, and other unmodeled effects. This procedure is done by using SSM/I measurements in known cloud-free areas. The reason for exploiting such measurements is that three unknown variables, i.e., the liquid water path, $\kappa_{\ell 19}$, and $\kappa_{\ell 37}$, can be eliminated from the model so as to provide a calibration that is independent of cloud properties [e.g., *Petty*, 1990]. The cloud-free data set consists of 12,287 individual SSM/I pixels that are considered to be, for the most part, free of cloud contamination based on Geostationary Operational Environmental Satellite (GOES) imagery [see *Petty*, 1990]. These observations are located primarily off the east and west coasts of the United States for August and September 1987 and January 1988. A number of additional pixels are also included from the North Sea for October 1987. This data set, unfortunately, represents a somewhat limited range of meteorological conditions with surface wind speeds ranging from 0 to 16 m s^{-1} and water vapor amounts mostly confined to less than 25 kg m^{-2} and extending only to about 50 kg m^{-2}. However, the monthly mean SSTs have a broad range from 275 to over 300 K.

Since the cloud liquid water for these observations is at or near zero, we can set $L = 0$ in (6) so that the water vapor optical depth at 37 GHz (τ_{w37}) is simply equal to τ_2. If τ_{w37} derived from the cloud-free data set is plotted against the PWC retrieved from (5), one can obtain a direct estimate of κ_{w37}. The relationship between τ_{w37} and PWC, as shown in Figure 3, is very distinct and nearly linear. A correction factor of 3.58 K was used in both 37-GHz channels to correct a constant offset that was evident in the optical depths. This factor is determined specifically for the SSM/I on the DMSP F-8 satellite and a recalibration of the model will likely be necessary for the SSM/Is on the other satellites. The rationale for adjusting these channels is that it is likely that the biases in the model are largely attributed to systematic biases in the 37-GHz brightness temperatures. This assumption is supported by the study of *Petty* [1990] where evidence of a cold bias of about 3 K in 37-GHz observations of melt-

TABLE 1. Cubic Fit Coefficients for Oxygen Transmission $\mathcal{T}_{ox}$ and Liquid Water Absorption κ_ℓ [from *Petty*, 1990] at 19.35 and 37 GHz

	a	b	c	d
$\mathcal{T}_{ox19}$	0.978	-6.31×10^{-5}	7.75×10^{-6}	-1.00×10^{-7}
$\mathcal{T}_{ox37}$	0.927	-8.53×10^{-5}	1.81×10^{-5}	-2.01×10^{-7}
$\kappa_{\ell 19}$	0.0786	-2.30×10^{-3}	4.48×10^{-5}	-4.64×10^{-7}
$\kappa_{\ell 37}$	0.267	-6.73×10^{-3}	9.75×10^{-5}	-7.24×10^{-7}

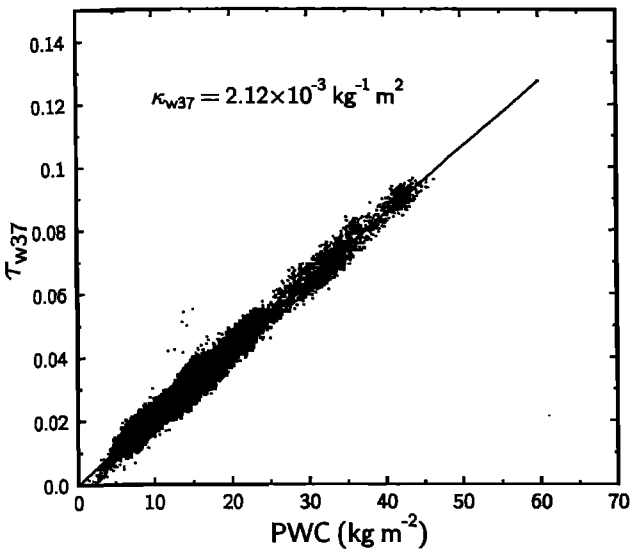

Fig. 3. Scatter diagram of total water vapor optical depth at 37 GHz (τ_{w37}) versus PWC (kg m^{-2}) derived from the cloud-free data set. Also shown is a linear least squares fit of the data where the slope corresponds to the water vapor absorption coefficient at 37 GHz (κ_{w37}).

ing snow was seen, suggesting that it is a sensor calibration error. *Petty* [1990] also independently derived a similar bias correction for the 37-GHz channels but expressed it as a correction to the sea surface emissivity. From a linear least squares fit, κ_{w37} is determined to be 2.12×10^{-3} kg^{-1} m^2. This is in reasonable agreement with the value of 2.0×10^{-3} kg^{-1} m^2 found by *Liu et al.* [1992], which was based on transmission calculations for 609 radiosonde soundings.

To illustrate how well the physical model behaves in regions of clear skies, a histogram is presented in Figure 4 of the cloud liquid water derived from the cloud-free data set. As expected, the mean LWP is near zero (3×10^{-4} kg m^{-2}), which is naturally a consequence of the calibration. What is more important, however, is the very small variability of the LWP, which has a standard deviation of 0.016 kg m^{-2}. This variability provides an observational measure of the minimum uncertainties that one might expect in the liquid water retrieval. It should be emphasized that the clear sky data set used in this study is a limited sample of observations and is weighted heavily toward low PWCs. Therefore in a tropical environment the value of κ_{w37} may require a slight adjustment and, as will be discussed in a subsequent section, the uncertainties in the retrieval are likely to be larger than 0.016 kg m^{-2}

4. VALIDATION

The strategy we have adopted to verify the retrieved liquid water involves a comparison to independent measurements of liquid water from ground-based microwave radiometers. One might say that a comparison of this type is simply an exercise in contrasting one passive microwave sensing technique to another and does not represent a validation. We argue, however, that observations from upward looking dual-frequency microwave radiometers, if they are well calibrated, are sufficient to operate as "ground truth." Ground-based methods can be, in principle, more accurate than satellite-based methods since the cosmic background is much colder (~3 K) and more stable than the ocean background, which is typically about 140 K at 37 GHz (53° zenith angle), for example, and can vary by 15 K or more. The theoretical study of *Westwater* [1978] demonstrated that dual-frequency ground-based microwave systems are able to provide cloud liquid water estimates with relative errors of less than 15% under a variety of conditions. *Albrecht et al.* [1990] showed for marine stratocumulus clouds over San Nicolas Island that ground-based measurements compared exceptionally well to adiabatically derived liquid water contents. An important point to emphasize, however, is that even ground-based measurements of liquid water can exhibit significant biases if one does not properly account for the contributions from oxygen and water vapor.

Comparisons of ground-based observations of cloud liquid water to in situ measurements from aircraft have also yielded good results [*Hill*, 1991, 1992]. The measurements of Hill, however, were made under special meteorological conditions in which the clouds were composed entirely of supercooled drops. *Petty and Katsaros* [1992*b*] compared in situ aircraft observations of liquid water to coincident measurements obtained from the SMMR on Nimbus 7 during the 1987 Taiwan Area Mesoscale Experiment. The comparison was surprisingly good, but the authors were cautious about making any definite conclusions because of the significant differences in sampling and the potentially large errors.

Visible Reflectance Method

The technique to estimate integrated cloud liquid water from reflectance measurements in the visible spectrum is based on the shortwave parameterization scheme of *Stephens* [1978], which relates the albedo of water clouds to their LWP. Coakley and Snider [unpublished manuscript, 1990] obtained a fit to the results of Stephens to yield a relationship between cloud albedo and LWP. This relationship is

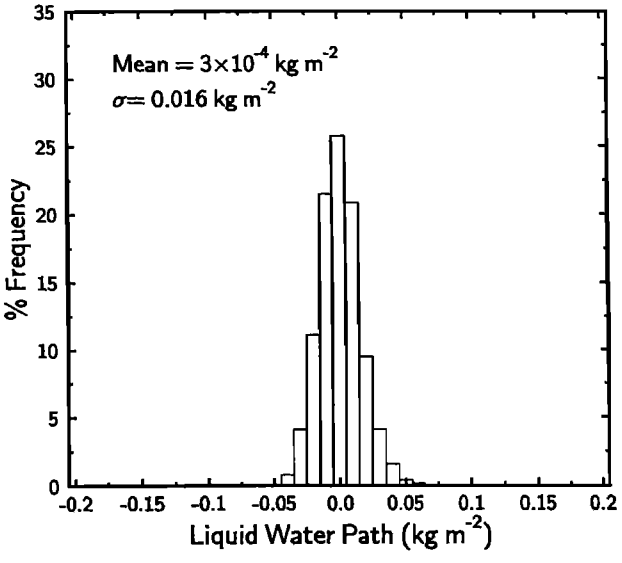

Fig. 4. Histogram of integrated cloud liquid water (kg m^{-2}) retrieved from the cloud-free data set. The mean and standard deviation are also indicated.

inverted to yield an expression for the liquid water path as a function of cloud albedo:

$$L = \frac{\mu_o RA}{1 - RB} \tag{9}$$

where μ_o is the cosine of the solar zenith angle, R is the cloud albedo, $A = 0.0490$, $B = 1.004$, and the liquid water path L is in units of kg m^{-2}. The standard deviation of the LWP can be approximated as

$$\sigma_L \approx \sigma_R \frac{\partial L}{\partial R} = \frac{\sigma_R \mu_o A}{(1 - RB)^2} \tag{10}$$

where σ_R is the cloud albedo standard deviation.

Visible reflectance measurements were obtained from the AVHRR aboard the NOAA 9 and NOAA 10 satellites. The channel of the AVHRR relevant to this study (channel 1) has a bandwidth ranging in the visible from 0.58 to 0.68 μm and a spatial resolution of 1 km at nadir. The AVHRRs on these satellites have exhibited a loss in sensitivity over the course of their lifetimes. The calibration factors used to correct this degradation are discussed by Coakley and Snider.

The comparison between the AVHRR-derived and the SSM/I-derived LWPs are confined to stratocumulus clouds over San Nicolas Island for July 1987. In each of the cases there is no precipitation, the clouds are, for the most part, single layered, and the cloud cover is complete over the island. Table 2 shows the NOAA 9, NOAA 10, and DMSP satellite overpass times. Only DMSP overpasses within about 4 hours of the NOAA overpasses are used, which is reasonable since marine stratocumulus cloud decks are relatively persistent features over the course of a few hours. The measurements from the NOAA satellites are taken within a 90-km radius of San Nicolas Island. Since the spatial resolution of the SSM/I is far cruder than the AVHRR, a radius of 75 km is used instead for the SSM/I observations.

Figure 5 shows a scatter plot of the SSM/I-derived LWP versus that estimated from the AVHRR. The error bars refer to the spatial variability of the measurements in terms of one standard deviation above and below the data points. The standard deviations for the AVHRR-derived LWP are calculated using (10). From Figure 5 it can be seen that the two methods give consistent results, with the SSM/I LWPs being offset higher than the AVHRR-derived LWPs. The rms difference is about 0.06 kg m^{-2}. This offset is likely due to the choice of the calibration factor that is used and presumably dominates over the effect of the disparity in the spatial resolutions of the two instruments. Apart from the offset the differences between the two methods might be caused by changes in the microphysics of the cloud that may have occurred between the DMSP and the NOAA satellite overpasses.

Ground Radiometer Observations

The ground radiometer measurements used in this study are taken from three island sites and one ship location. Although this is a very small sample of sites, they do represent various seasons and climate regimes. One disadvantage of using island locations is that they might contaminate the retrievals. Fortunately, most of the islands are comparatively small and the satellite footprints are large enough so that they produce a small to negligible effect on the SSM/I brightness temperatures. The possible exception is San Nicolas Island, which may cause a nonnegligible increase in the 37-GHz channels if the island is within a large fraction of the FOV of the instrument.

TABLE 2. Selected Cases for the AVHRR and SSM/I Cloud Liquid Water Comparison Over San Nicolas Island

	NOAA 10		DMSP	
Case	Date	UT	Date	UT
1	July 10	1537	July 10	1320
2	July 16	1647	July 16	1348
	NOAA 9		DMSP	
Case	Date	UT	Date	UT
3	July 15	2256	July 16	0226
4	July 16	2246	July 17	0213

AVHRR, advanced very high resolution radiometer; SSM/I, special sensor microwave/imager.

The major obstacle in directly comparing ground observations to satellite observations is of course the significant differences in sampling of the two measurement systems. In our opinion the most useful way of comparing these measurements is through the use of histograms. For the SSM/I data, spatial histograms are constructed from pixels that are within 50 km of the site. Unless otherwise noted, temporal histograms are derived from the ground observations over a 1-hour time period centered on the time of the satellite overpass.

In the first comparison, measurements of integrated cloud liquid water are used from a surface-based microwave radiometer on San Nicolas Island (33.25°N, 119.6°W) during the First ISCCP Regional Experiment (FIRE). The radiometer has three channels at 20.6, 31.65, and 90 GHz. The integrated water vapor and liquid water are estimated simul-

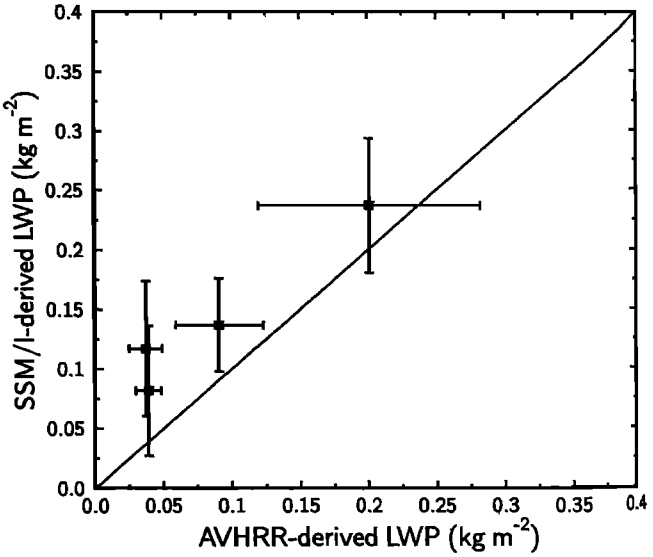

Fig. 5. Scatter diagram of cloud liquid water path (kg m^{-2}) derived from the present method (SSM/I) versus that determined from the visible reflectance method (advanced very high resolution radiometer (AVHRR)) over San Nicolas Island. Error bars about these points represent the spatial variability of the measurements and are one standard deviation above and below the points.

taneously from a statistical retrieval algorithm discussed by *Hogg et al.* [1983] and the errors in the liquid water are estimated at 20%.

The San Nicolas Island comparison involves nine cases. All but two cases consist of overcast conditions as determined from ceilometer measurements [*Schubert et al.*, 1987]. The July 13 case is free of clouds, while the July 18 case has broken cloud conditions. As depicted in Figure 6, the agreement between the two different sets of observations is remarkable. To provide a rough quantitative estimate of the disparity between these data sets, the temporal mean value for the ground observations and the spatial mean value for the SSM/I data are computed for each case. It is found that the overall rms difference between the surface-based and SSM/I mean values is 0.036 kg m^{-2}. It is probable that the underestimation by the SSM/I for the July 16 case is linked to an error in the cloud temperature, which becomes increasingly important for higher liquid water amounts. Ceilometer measurements indicate during this time that the cloud deck was low, with a cloud base at about 200 m, so the specified cloud temperature may indeed be too cold. The July 18 case has the SSM/I generally overestimating the liquid water for a thin, broken cloud deck. Under these conditions one would expect the SSM/I to underestimate the cloud water. The likely explanation is that several of the outermost pixels are sensing a thicker portion of the cloud deck that was evident earlier in the ground observations from 1145 to 1245 UT.

The second set of ground-based measurements originate from Kwajalein Island (8.7°N, 167.75°E) in the West Pacific during March and April 1988. These measurements were estimated from two different microwave radiometers: the University of Massachusetts autocorrelation radiometer (CORRAD) that measures downwelling radiation at 31 channels from 20.5 to 23.5 GHz and an additional radiometer that only senses radiation at 37 GHz. The method of retrieving both water vapor and cloud liquid water involves the 21-, 22.2- and 37-GHz channels based on a statistical minimum error technique [*Alishouse et al.*, 1990].

The most consistent feature of the comparison in Figure 7 is that the SSM/I frequently underestimates the liquid water, with the worst case occurring at 1830 UT on March 29. The rms difference between the mean values is 0.13 kg m^{-2}. These differences are too great to be caused entirely by errors in cloud temperature because a temperature warmer than the surface temperature would be needed to bring the two observations into agreement. Uncertainties in modeling the surface or geolocation errors of the SSM/I, which were common from July 1987 until the end of 1988, may also contribute to this difference. Another possibility is that if the cloudiness is patchy or the clouds are very inhomogeneous, this may cause the SSM/I to underestimate the LWP.

For the March 26 Kwajalein Island case a qualitative comparison is made in Plate 1 of the cloud liquid water field derived from the SSM/I to visible satellite imagery. The visible image is taken from the AVHRR on board the NOAA

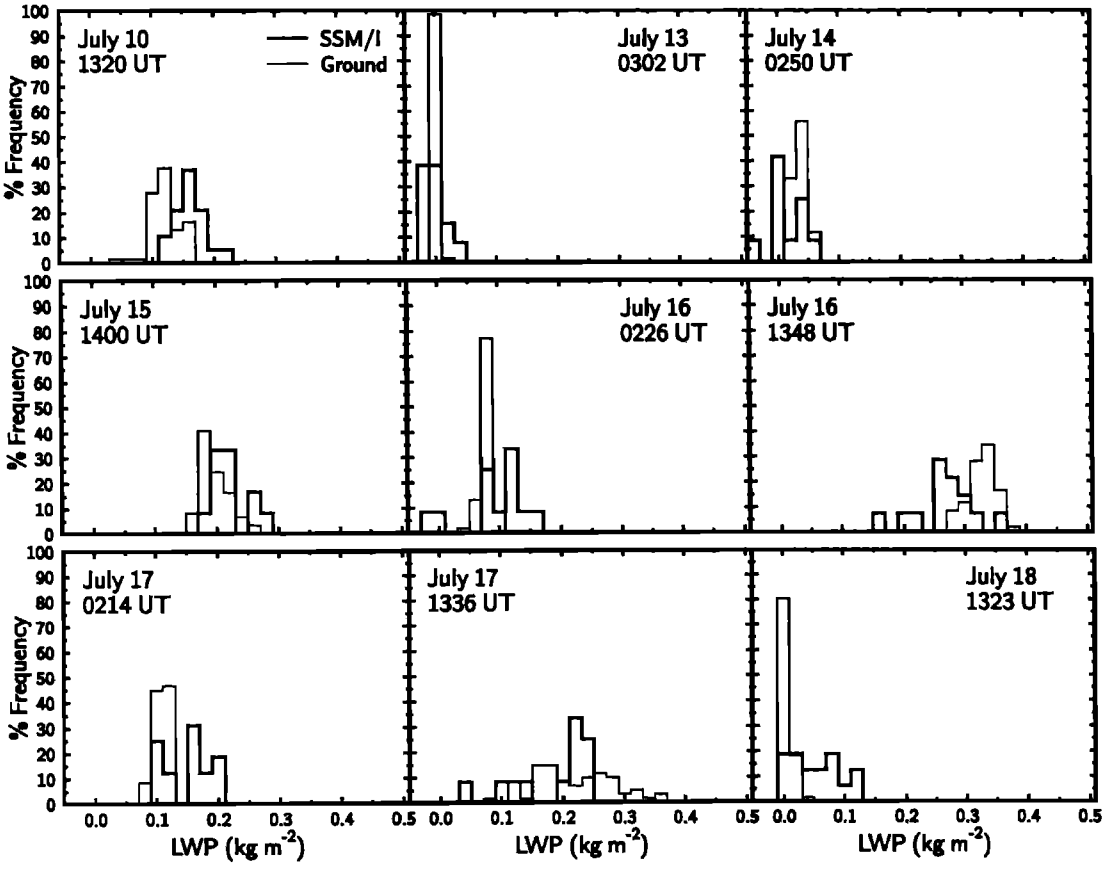

Fig. 6. Comparison of histograms of LWP (kg m^{-2}) from the SSM/I and ground observations for cases in July 1987 over San Nicolas Island.

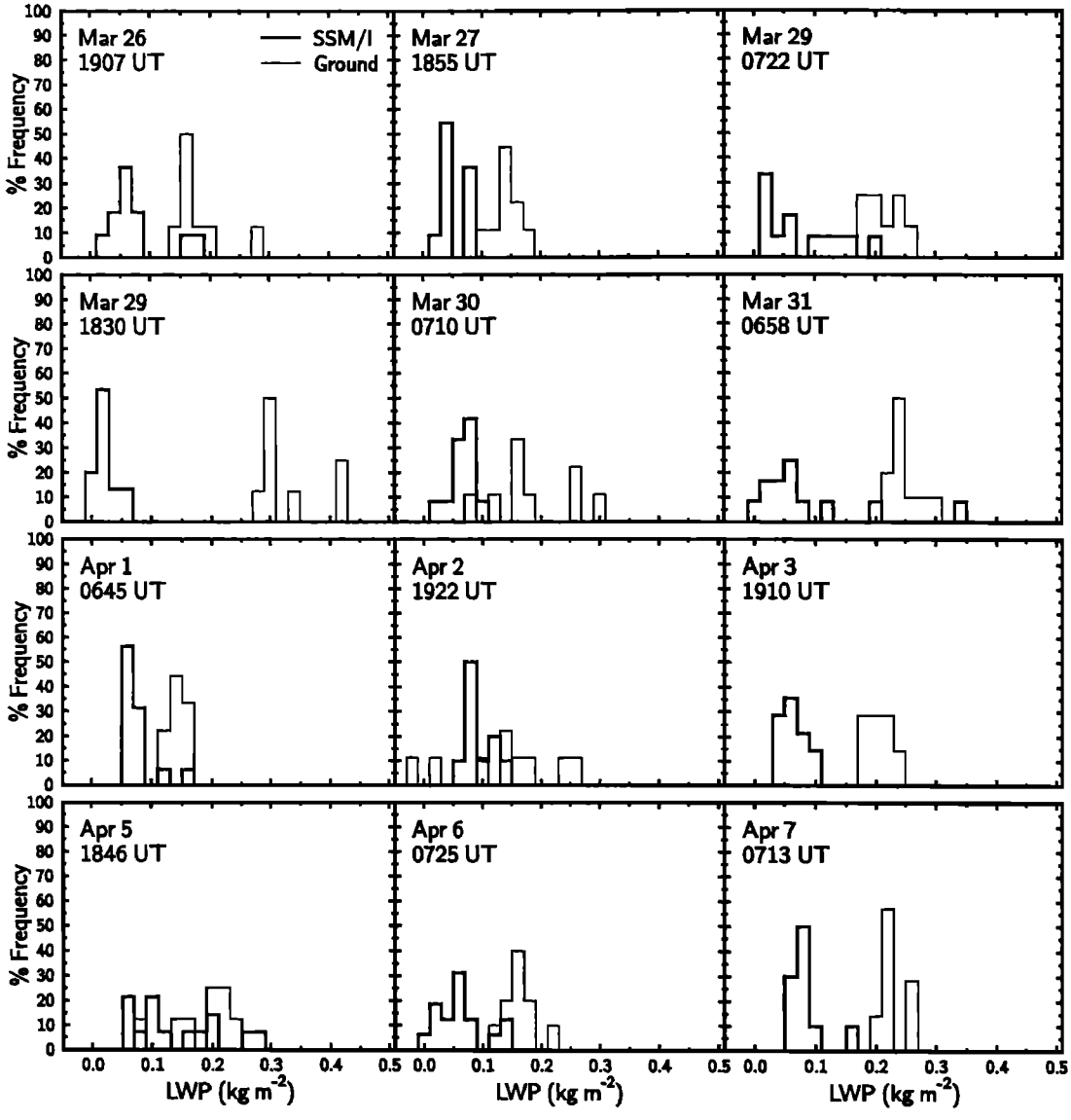

Fig. 7. Comparison of histograms of LWP (kg m^{-2}) from the SSM/I and ground observations for cases in March and April 1988 over Kwajalein Island.

10 satellite, which passed over the island at roughly 2000 UT. Also shown is the cloud liquid water field on a pixel scale for a portion of the DMSP orbit at 1907 UT. Values of LWP greater than 0.5 kg m^{-2} are portrayed as a gray tone. The most distinctive feature in both the satellite imagery and the cloud liquid water field is the long band of convection located south of the island near the equator. Nearly all LWPs in this region extend beyond 0.5 kg m^{-2} and indicate possible heavy and widespread rainfall. In other areas a good correspondence can be seen between other smaller individual cloud systems and the liquid water field.

The third group of measurements were made in the North Sea in October 1989 during the International Cirrus Experiment (ICE) on the R/V *Poseidon*. The microwave radiometer was supplied by the University of Hamburg in Germany and operates at a frequency of 33 GHz. The method used to determine cloud liquid water is briefly described by *Hargens* [1992] and has an estimated minimum error of 0.06 kg m^{-2}.

A number of selected cases at this site are shown in Figure 8. Cases that were suspected of being contaminated by precipitation are excluded from the comparison. The agreement between the two data sets is generally very good, with the tendency of the SSM/I to slightly overestimate the LWP, especially for higher amounts. The rms difference for all the cases is 0.046 kg m^{-2}. It is not known whether the differences are a consequence of improper specification of the sea surface and/or cloud temperature. For higher liquid water amounts the cause may be related to the cloud temperature.

The final set of measurements were carried out during the TCM experiment in August and September 1990 on Saipan Island (15.2°N, 145.8°E) in the West Pacific. These measurements were provided by the Penn State nine-channel microwave radiometer. The retrieval of cloud liquid water involves a physical inversion method [*Westwater*, 1978] and includes ceilometer measurements of cloud base height to help improve estimates of the cloud absorption [*Han and Thomson*, 1992]. The errors are roughly 5% based on theoretical calculations.

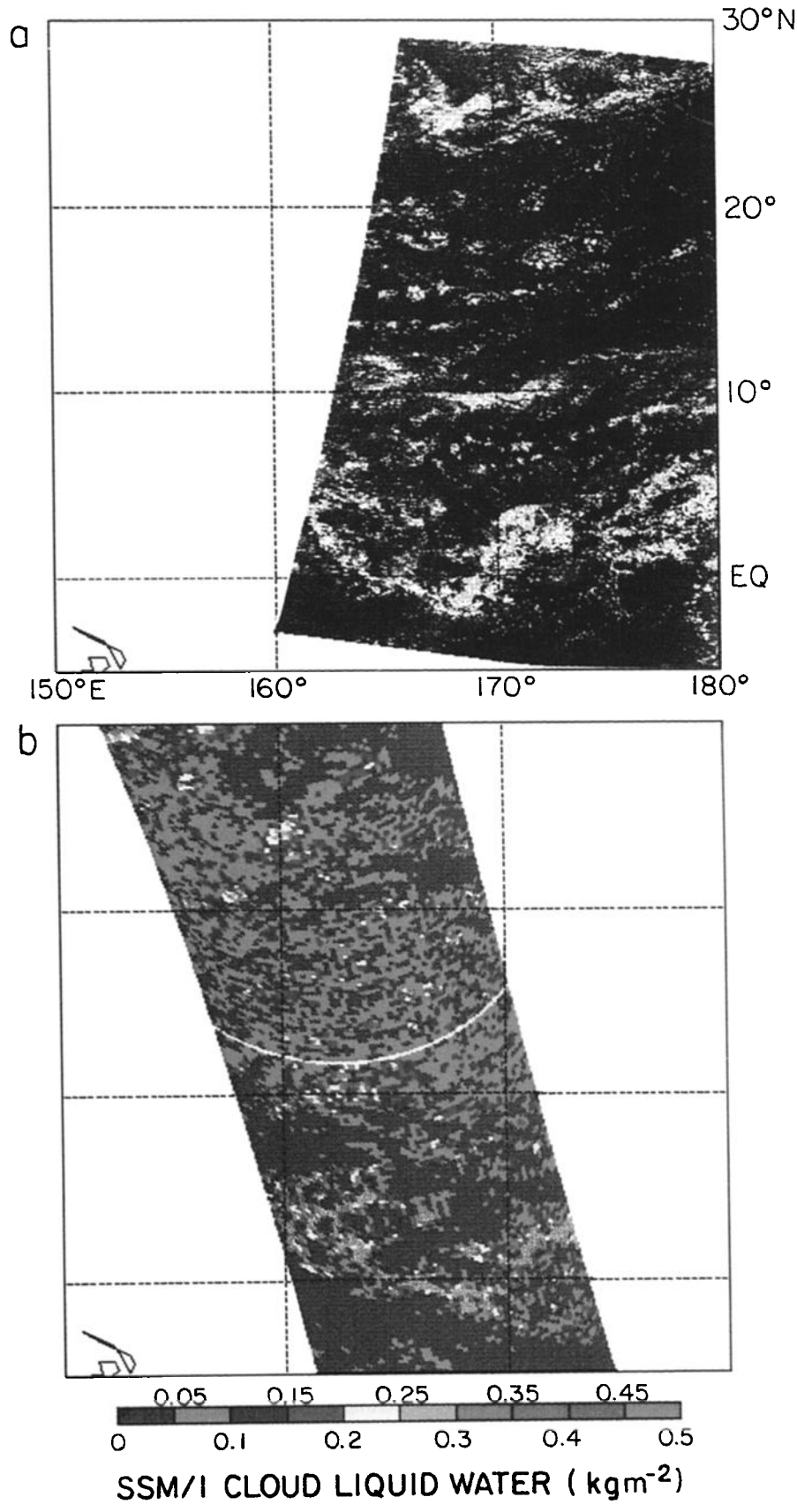

Plate 1. (a) NOAA 10 visible image over Kwajalein Island for March 26, 1988, at 2000 UT. (*b*) SSM/I-derived cloud liquid water field for the same day at 1907 UT. Gray areas denote where LWP > 0.5 kg m^{-2}.

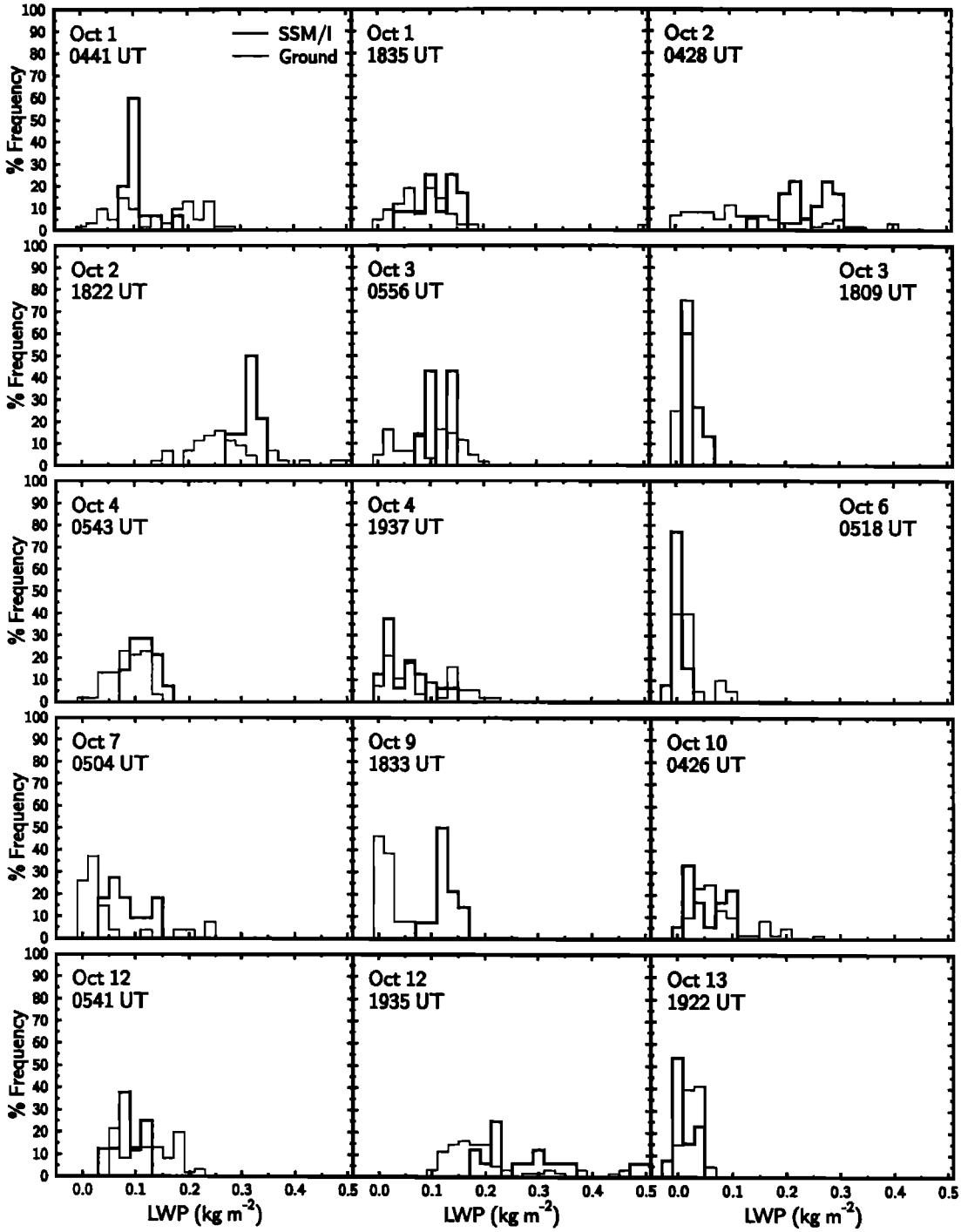

Fig. 8. Comparison of histograms of liquid water path (LWP) (kg m^{-2}) from the SSM/I and ground observations for cases in October 1989 in the North Sea.

The results of the analysis for selected cases are presented for August and September in Figure 9. Ceilometer measurements on Saipan Island are used to exclude cases where precipitation is occurring since both surface- and satellite-based methods are sensitive to moderate and heavy rain. For this set of ground observations the histograms are created from a 2-hour time interval centered about the satellite overpass time. There appears to be a qualitative consistency between the two data sets, although it is difficult to evaluate this agreement because of the greater variability of the SSM/I-derived LWPs.

A comparison of specific interest is the September 7 morning case (2015 UT). During this time it is likely that a thin stratiform-type cloud deck is overlaying the island since a time series of the surface observations shows that the cloud liquid water is relatively uniform (0.15 – 0.2 kg m^{-2}) over a period of 5 hours. Unfortunately, measurements of the cloud base height are not available to confirm that these clouds are stratiform in nature. As shown in Figure 9, both sets of measurements appear to be in reasonable agreement with one another, where the SSM/I slightly underestimates the LWP.

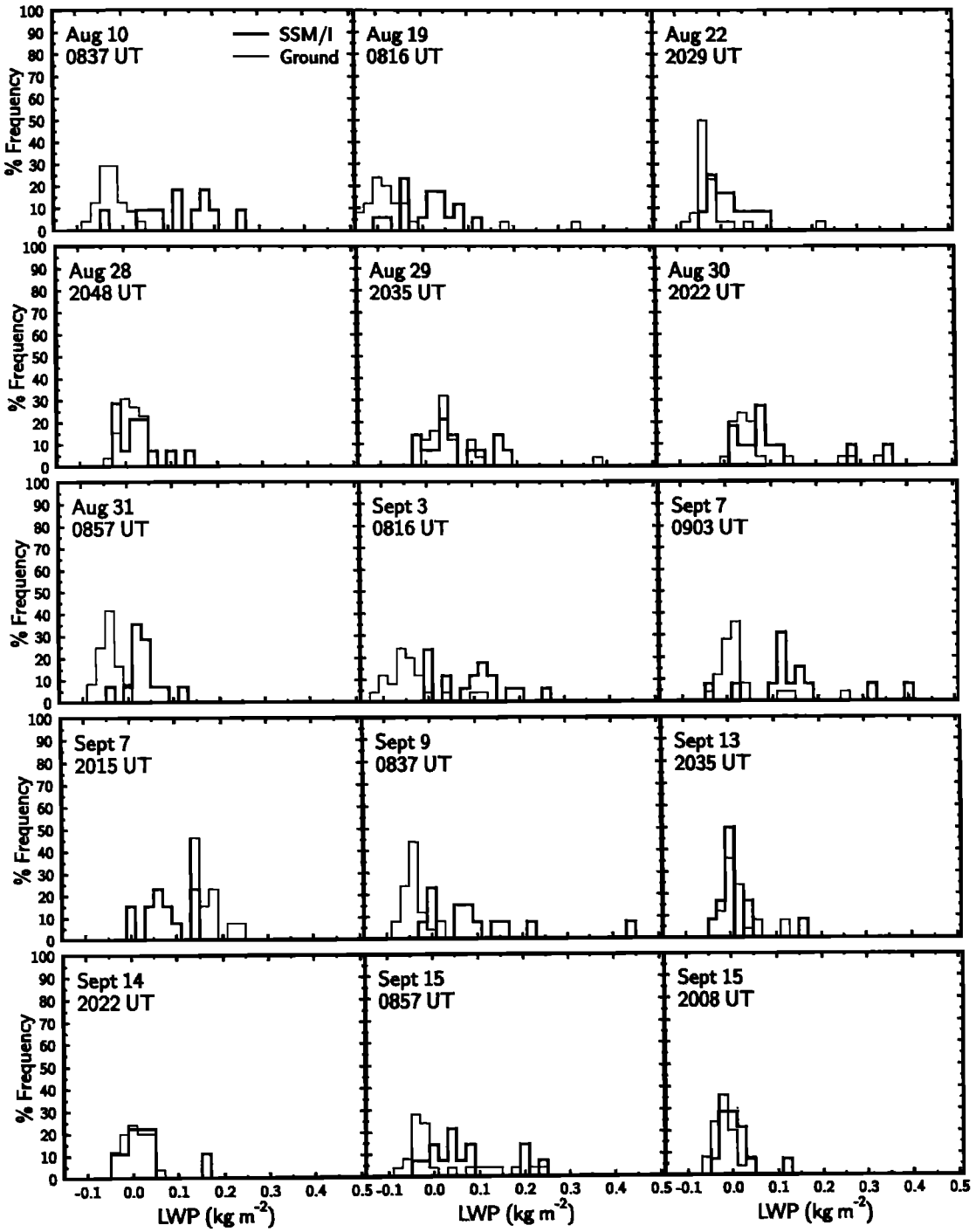

Fig. 9. Comparison of histograms of LWP (kg m^{-2}) from the SSM/I and ground observations for cases in August and September 1990 over Saipan Island.

One characteristic of the surface measurements of cloud liquid water on Saipan Island that prevents a more thorough analysis of the two data sets is the existence of an obvious negative bias. For instance, on August 31 where the skies are mostly clear, the ground observations show a mean LWP of -0.047 kg m^{-2}. In another case on September 17 (not shown in Figure 9), where high clouds are present (the ceilometer measurements indicate cloud bases at 2 and 3.5 km), the ground observations have a mean LWP of -0.055 kg m^{-2}. Unfortunately, the bias does not appear to be systematic and its cause is largely uncertain. One can conclude from this comparison that it is extremely difficult to get reliable estimates of LWP from both satellite and ground observations in the tropics. Thus there is a need for high-quality surface measurements of cloud liquid water in areas such as the tropical West Pacific.

Other Special Sensor Microwave/Imager (SSM/I) Methods

The present method is now compared to other cloud liquid water retrieval schemes that have been developed for the SSM/I. The comparison involves the algorithms of *Petty*

[1990], *Alishouse et al.* [1990], and *Hargens* [1992] in two specific regions.

Our first area of interest is the stratocumulus cloud decks that regularly form off the west coast of North America. We confine the analysis to an area bounded from 25° to 40°N latitude and from 118° to 130°W longitude over the time period July 16–18, 1987. The semiphysical method of *Petty* [1990] involves a parameterization based on the cloud-free data set described earlier and whose coefficients were determined specifically from the water vapor algorithm given by *Petty* [1990] and for the wind speed algorithm of *Goodberlet et al.* [1989]. This method is intended for use with spatially smoothed fields of W and wind speed, although this was not done in the present comparison. An alternative four-channel algorithm to the one presented by *Alishouse et al.* [1990] is also used in the comparison, where the 37h channel replaces the 85h channel (J. C. Alishouse, personal communication, 1991).

The results of the comparison, which were done on a pixel basis, are depicted in Figure 10. A cloud temperature of 285 K was specified for both the Petty algorithm and the present method. Good agreement can be seen in Figure 10*a* between the physical methods. The rms difference is only 0.027 kg m^{-2}, but there is some discrepancy for lower liquid water amounts. In the comparison to *Alishouse et al.* [1990] in Figure 10*b*, more significant differences are evident. The statistical method has an rms difference of 0.074 kg m^{-2} and severely underestimates the LWP by roughly a factor of 2 for all values. Although the method of Alishouse et al. appears to have the ability to at least partially detect a cloud liquid water signal, the primary reason for the discrepancy is that the influence of water vapor has not been fully separated from the effects of clouds. This fact is confirmed by *Petty* [1990] who observed that the Alishouse et al. LWPs were highly correlated with water vapor.

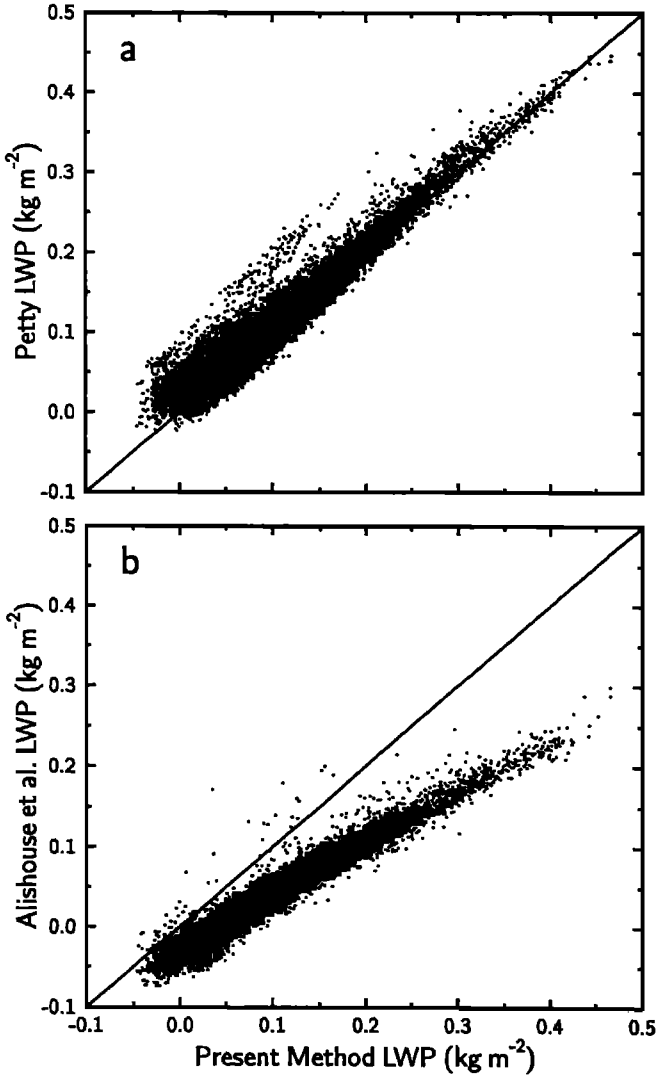

Fig. 10. Scatter diagrams of LWP (kg m^{-2}) derived from the method of (*a*) *Petty* [1990] and (*b*) *Alishouse et al.* [1990] versus the present method for stratocumulus clouds off the west coast of California from July 16 to 18, 1987.

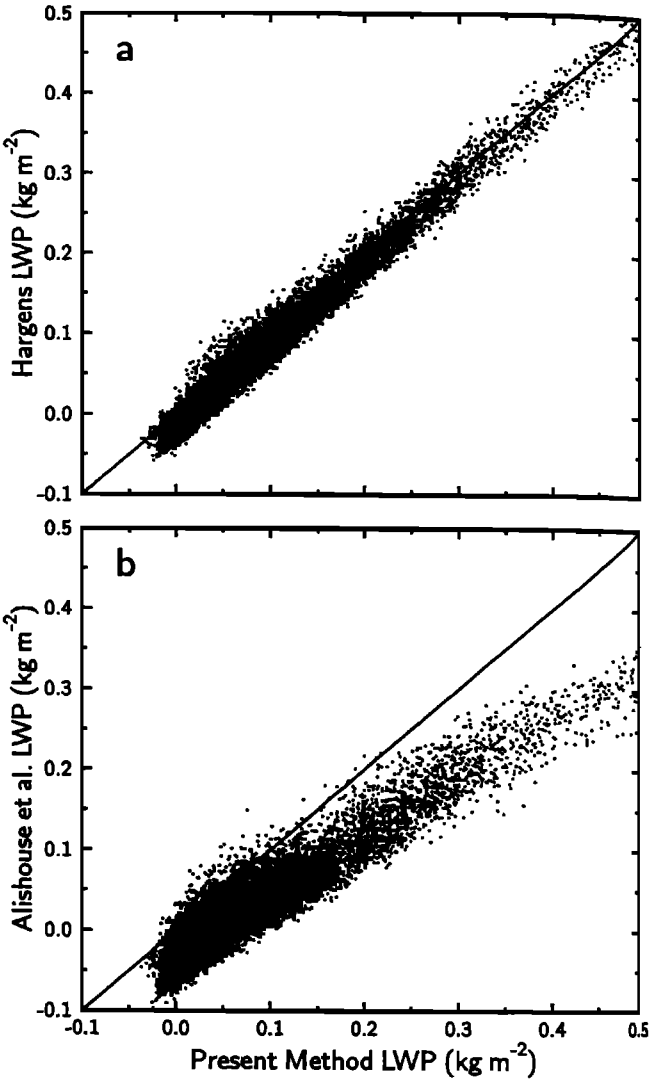

Fig. 11. Scatter diagrams of LWP (kg m^{-2}) derived from the method of (*a*) *Hargens* [1992] and (*b*) *Alishouse et al.* [1990] versus the present method over the North Sea from October 1 to 18, 1989.

The next region for comparison is the North Sea from October 1–18, 1989 during ICE. The area that is defined is from 54.5° to 58°N and from Greenwich to 5.7°E. The LWP retrieval method of Hargens is based on theoretical calculations for roughly 3000 radiosonde profiles in the North Sea

and Atlantic Ocean. Multiple regression is then used to relate the computed brightness temperatures to the cloud liquid water prescribed in the model.

The comparison between the present model and the Hargens algorithm for the North Sea is shown in Figure 11*a*. Excellent agreement can be seen except that the LWPs derived from the present retrieval method are offset slightly higher. The rms difference between these data sets is 0.019 kg m^{-2}. The small differences may be explained by a small negative bias of about 0.02–0.025 kg m^{-2} in the LWP's from the method of Hargens, which was determined from the cloud-free data set for the North Sea observations. The algorithm of *Alishouse et al.* [1990] in Figure 11*b* has an rms difference of 0.073 kg m^{-2} and again underestimates the LWP with a large fraction of values less than zero.

5. Sensitivity and Error Analysis

In this section the aim is to provide quantitative estimates of the relative retrieval errors under different meteorological conditions. The analysis is confined to nonprecipitating clouds. The approach that is used to determine the errors in (8) is one based on propagation of errors, whereby the variance in L can be expressed as a sum of the uncertainties in a few key atmospheric and surface variables as

$$\sigma_L^2 \approx \sigma_u^2\left(\frac{\partial L}{\partial u}\right)^2 + \sigma_{T_c}^2\left(\frac{\partial L}{\partial T_c}\right)^2 + \sigma_{T_s}^2\left(\frac{\partial L}{\partial T_s}\right)^2 + \sigma_{T_b}^2\left(\frac{\partial L}{\partial T_b}\right)^2 + \sigma_{\kappa_w}^2\left(\frac{\partial L}{\partial \kappa_w}\right)^2 + \sigma_{T_{ox}}^2\left(\frac{\partial L}{\partial T_{ox}}\right)^2 \quad (11)$$

where u is the near-surface wind speed, T_b represents the brightness temperatures, and σ is the standard deviations of the respective parameters. It is assumed in (11) that there is little or no correlation among the variables so the covariances are negligible. Uncertainties in the SSM/I incidence angle are neglected because their influence on the results are of the order of only a few percent.

The uncertainty in L will, of course to a large extent, depend on what values are designated for the uncertainties in the various independent variables in (11). A pessimistic value of ±4 m s^{-1} is assigned to the uncertainty in the surface wind speed, which is a factor of 2 larger than the error quoted by *Goodberlet et al.* [1989] for the wind speed algorithm. The error in using a monthly mean SST is assumed to be ±3 K in the tropics and midlatitudes. A larger uncertainty of ±4 K is specified for the higher latitudes. A reasonable uncertainty of ±10 K is given to the cloud temperature and the noise in the four SSM/I channels is set to a value of 0.5 K. Since uncertainties in the water vapor absorption coefficients are difficult to assess, they are given an arbitrary error of 5%. Finally, the errors associated with the oxygen transmittance are based on a 5% uncertainty in the absorption.

Table 3 shows the results of the error analysis for a tropical (SST = 300 K, W = 50 kg m^{-2}), midlatitude (SST = 294 K, W = 30 kg m^{-2}), and high-latitude (SST = 277 K, W = 10 kg m^{-2}) atmosphere as a function of LWP. A surface wind speed of 6 m s^{-1} is used in the calculations. The most obvious behavior of the errors is that the smallest percentage errors of about 24% occur for the largest LWPs. These errors are largely controlled by uncertainties in cloud temperature.

To examine the relative contribution of each of the variables to the total error, the quantity $\sigma_x \partial L/\partial x$ was computed for each variable x and the results are shown in Table 4. It can be seen from this table that the errors in cloud temperature increase dramatically for increasing cloud liquid water. Thinner clouds, on the other hand, have higher percentage errors ranging from about 30% to 50%, which are primarily dictated by errors in T_s and u for a drier atmosphere. For greater water vapor there are also significant contributions from brightness temperature noise and to uncertainties in the water vapor absorption coefficients, since they are directly related to the atmospheric optical thicknesses, τ_1 and τ_2. Although not shown in Table 4, the errors decrease slightly for higher wind speeds. What is clear from this analysis is that the retrieval errors vary greatly depending on the surface and atmospheric conditions, with the largest errors occurring in a tropical atmosphere.

There are many other potential sources of error that are not considered in (11). These include, for instance, unmodeled effects such as variations in temperature, humidity, and cloud liquid water profiles, although the effect of temperature profile variability on the oxygen transmittance is ac-

TABLE 3. Theoretical Error Estimates in Terms of Standard Deviation (kg m^{-2}) of the Cloud Liquid Water Retrieval as a Function of LWP for Conditions of the Tropics (W = 50 kg m^{-2}, T_s = 300 K), Midlatitudes (W = 30 kg m^{-2}, T_s = 294 K), and High Latitudes (W = 10 kg m^{-2}, T_s = 277 K)

	Tropics		Midlatitudes		High Latitudes	
LWP, kg m^{-2}	σ_L	Error, %	σ_L	Error, %	σ_L	Error, %
0.0	0.044	–	0.031	–	0.025	–
0.1	0.051	51	0.039	39	0.033	33
0.2	0.065	33	0.057	28	0.053	27
0.3	0.084	28	0.078	26	0.076	25
0.4	0.10	26	0.10	25	0.10	25
0.5	0.13	25	0.12	24	0.13	25
0.6	0.15	25	0.15	24	0.15	25
0.7	0.17	24	0.17	24	0.18	25
0.8	0.19	24	0.19	24	0.21	26
0.9	0.21	24	0.22	24	0.23	26
1.0	0.24	24	0.24	24	0.26	26

LWP, liquid water path.

TABLE 4. Contributions of the Independent Variables to the Retrieval Errors (Units of kg m^{-2}) for Different Cloud Liquid Water Amounts and PWC Values of 10 and 50 kg m^{-2} Using a Near-Surface Wind Speed of 6 m s^{-1}

	$W = 10$ kg m^{-2}								
LWP, kg m^{-2}	u	T_c	T_s	T_{19v}	T_{37v}	κ_{w19}	κ_{w37}	$\mathcal{T}_{ox19}$	$\mathcal{T}_{ox19}$
0.0	0.014	0.0	0.015	−0.0057	0.0099	−0.0015	−0.0034	−0.0022	0.0084
0.1	0.014	0.024	0.0086	−0.0058	0.011	−0.0035	−0.0045	−0.0022	0.0084
0.5	0.014	0.12	−0.026	−0.0065	0.016	−0.012	−0.0087	−0.0022	0.0084
1.0	0.014	0.24	−0.093	−0.0075	0.025	−0.022	−0.014	−0.0022	0.0084
	$W = 50$ kg m^{-2}								
	u	T_c	T_s	T_{19v}	T_{37v}	κ_{w19}	κ_{w37}	$\mathcal{T}_{ox19}$	$\mathcal{T}_{ox19}$
0.0	0.015	0.0	0.0001	−0.012	0.017	−0.013	−0.030	−0.004	0.015
0.1	0.015	0.022	−0.0045	−0.012	0.018	−0.015	−0.031	−0.004	0.015
0.5	0.015	0.11	−0.026	−0.013	0.022	−0.023	−0.035	−0.004	0.015
1.0	0.015	0.22	−0.061	−0.014	0.029	−0.033	−0.040	−0.004	0.015

PWC, precipitable water content.

counted for in a crude way. Other errors can result from the spatial distribution and structure of the clouds. For example, if the cloud liquid water is vertically distributed in multiple layers or over a single deep layer, an effective cloud temperature alone may be inadequate to represent the cloud(s).

Additional, and possibly more significant, errors can arise from SSM/I footprints that are partially filled by clouds and by clouds that are markedly horizontally inhomogeneous. *Gagarin and Kutuza* [1983] examined the effect of broken cloudiness on microwave brightness temperatures at 22 and 37 GHz based on aircraft measurements over the ocean. They reported that an underestimation of the retrieved cloud liquid water occurs, particularly for cumuliform-type clouds, if broken cloudiness within the satellite footprint is not taken into account. *Jones and Vonder Haar* [1990] investigated the effect of cloudiness on LWP retrieval over land and found that the largest errors are associated with small liquid water amounts and sparse cloudiness. That study, however, involved the 85-GHz channels where nonlinearities caused by partial cloudiness and cloud inhomogeneities play a more important role in affecting the brightness temperatures than at 37 GHz.

Still other sources of error involve the sea surface emissivity model and possible effects from ice clouds. Because of the lack of observational studies, the influences of wind, foam, and other effects on the surface emissivity are not well known. Therefore it is not possible to address these errors in this study. As for clouds composed of ice, the optical depths are typically small outside areas of precipitation, so their effect on the brightness temperatures at 19.35 and 37 GHz will likely not be appreciable [*Petty and Katsaros*, 1992*a*], although thick anvil clouds in the tropics may have an impact on the 37 GHz channels.

One final source of error that is of concern is how the different footprint sizes at 19.35 and 37 GHz affect the retrieval. A quantitative estimate can be made of this error by using the approach of *Robinson et al.* [1992] to enhance the 19.35-GHz channels to the resolution of the 37-GHz channels. A segment of a DMSP orbit was arbitrarily selected for this analysis from 1508 to 1532 UT July 16, 1987, which extended from about 45°N to 45°S in the eastern Pacific. The rms error between the corrected and the uncorrected LWP retrievals was determined for three different PWC categories (< 15 kg m^{-2}, 25–35 kg m^{-2}, and 45–55 kg m^{-2}) that roughly correspond to the different atmospheric environments in Table 3. The error was found to increase from 0.012 kg m^{-2} for the driest atmosphere, to 0.017 kg m^{-2} for PWCs ranging from 25 to 35 kg m^{-2}, and 0.022 kg m^{-2} for the tropical atmosphere. A comparison to the results of Table 3 indicates that the error resulting from the spatial disparity between the 19.35- and the 37-GHz channels is far less than the errors arising from uncertainties in the atmospheric and surface variables.

6. RESULTS

The spatial characteristics of cloud liquid water over the oceans can now be examined using monthly mean global maps computed from the physical model. Plate 2 shows the integrated liquid water content derived from SSM/I data for the months of August 1987 and February 1988 presented on a 1° × 1° grid. From these distributions it can be seen that patterns of liquid water relate quite well to features of the general circulation. For instance, both seasons show the distinct signatures of the intertropical convergence zone (ITCZ), South Pacific convergence zone and northern midlatitude baroclinic regions, where the liquid water can sometimes reach 0.22 kg m^{-2} or more. In areas of persistent stratocumulus clouds off the west coasts of North and South America and Africa the liquid water amounts are generally smaller, typically ranging from 0.10 to 0.13 kg m^{-2}. The lowest values of cloud water (< 0.04 kg m^{-2}) are consistent with regions dominated by strong subtropical high-pressure systems over the summer oceans, which are observed in February, for example, off the west coast of Australia. Also seen in the month of February is the dramatic southward migration of the northern hemisphere storm tracks.

Although the present method appears to give reasonable patterns and magnitudes of liquid water on a monthly basis, it is useful to compare these distributions to previously published results. Figure 12 shows the latitudinal distribution of SSM/I cloud liquid water for August 1987 and liquid water from the study of *Njoku and Swanson* [1983]

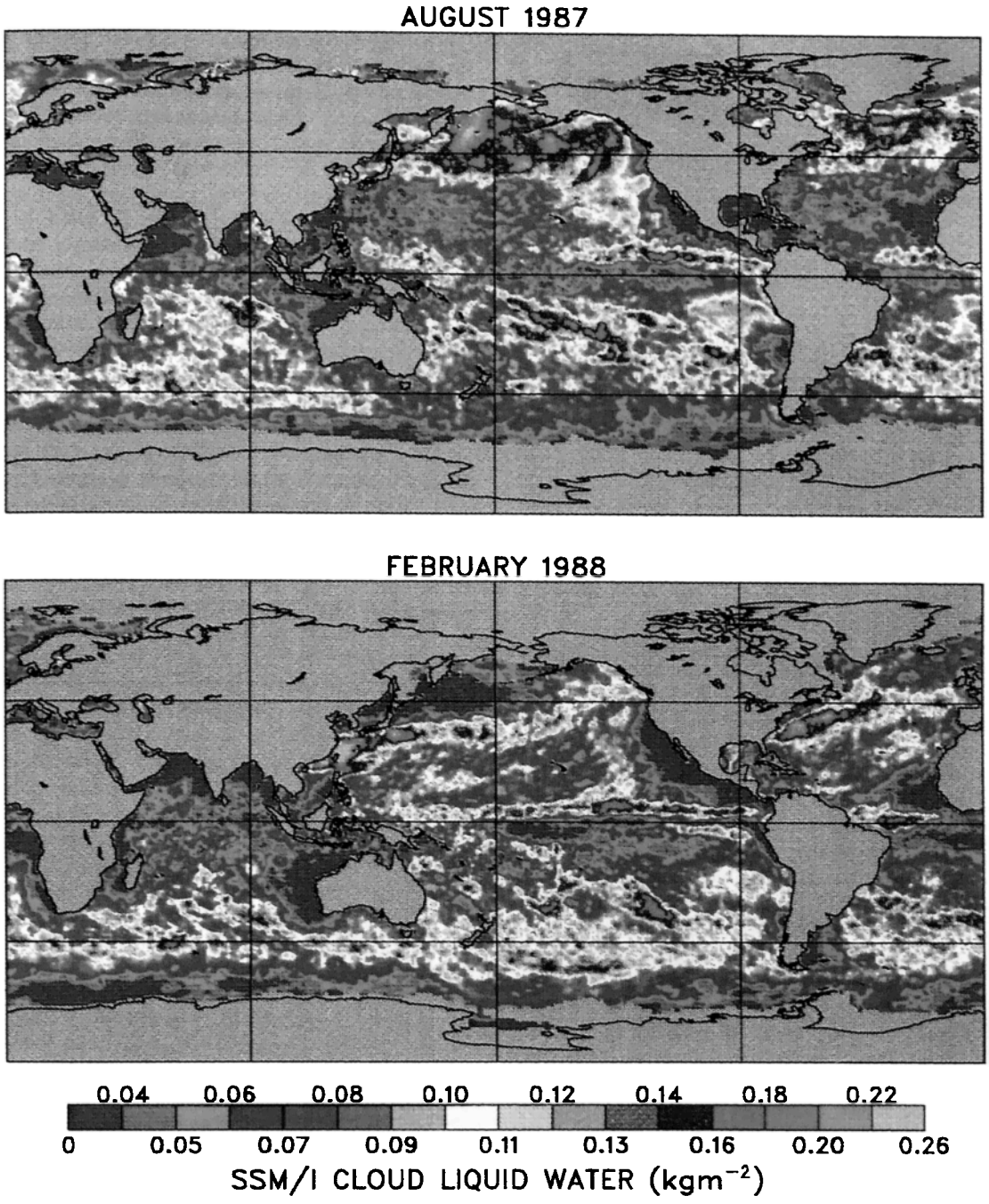

Plate 2. Monthly mean global distributions of cloud liquid water (kg m^{-2}) over the ocean derived from SSM/I measurements for (top) August 1987 and (bottom) February 1988.

for July 11-August 10, 1978 and the method of *Prabhakara et al.* [1983] for August 1979. There is a surprisingly good correlation in the latitudinal behavior of the liquid water between the present method and the results of Njoku and Swanson. The method used by Njoku and Swanson is based on SMMR observations made from the Seasat and consists of a slightly modified form of the statistical regression method of *Wilheit and Chang* [1980]. The magnitude of the SMMR results in the tropics and subtropics appears to be biased slightly lower than the SSM/I liquid water, which shows greater values in the ITCZ region. It is not known whether these differences are caused by the interannual variability of cloud liquid water, differences in temporal and spatial sampling between the SSM/I and SMMR, or simply by biases in either method. We speculate that some of these differences may be accounted for by the retrieval of cloud liquid water in areas of precipitation where the retrievals are less reliable. In any case, these differences are most likely within the errors associated with the SSM/I retrievals.

The comparison to the liquid water derived from the method of *Prabhakara et al.* [1983] reveals a reasonable correspondence in the equatorial region but far less agreement at higher latitudes. Their physical approach is based on measurements at 6.6 and 10 GHz from the Nimbus 7 SMMR and estimates the total liquid water content of the atmosphere, which includes contributions from both clouds

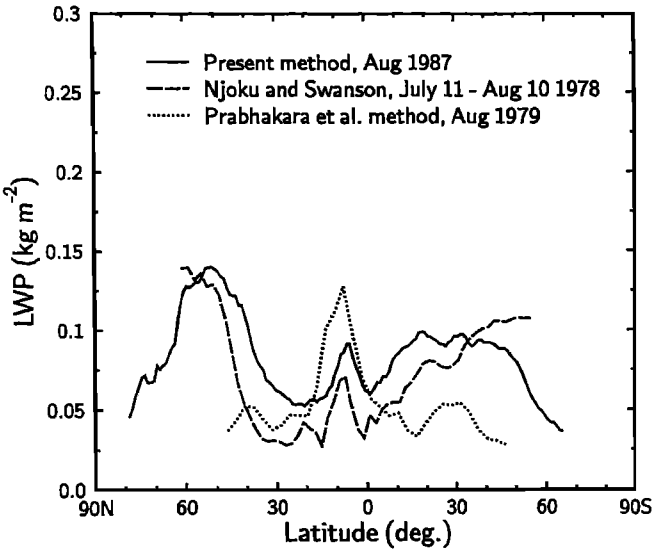

Fig. 12. Zonal distributions of cloud liquid water (kg m^{-2}) derived from the present method for August 1987 (solid), Seasat special multichannel microwave radiometer (SMMR) results from the study of *Njoku and Swanson* [1983] for July 11 to August 10, 1978 (dashed), and Nimbus 7 SMMR results from the method of *Prabhakara et al.* [1983] for August 1979 (dotted).

and precipitation. These frequencies are primarily sensitive to high amounts of liquid water, which are in the form of raindrops in the precipitating convective systems of the tropics. Thus the liquid water amounts retrieved from this method are more likely representative of rain water than cloud liquid water. This idea may explain why the liquid water has a significant maximum in the equatorial region and steadily decreases toward the poles, with relative maxima in the midlatitudes caused by the precipitation in cyclonic storms (the low values in the subtropics and midlatitudes are also caused by the inability of the algorithm to estimate cloud liquid water in regions of low-level divergence, where marine stratocumulus clouds commonly form). Further evidence for this interpretation is supported by the rainfall study of *Prabhakara et al.* [1986] where these same liquid water fields were used to derive rainfall climatologies because of their close resemblance to spatial distributions of rainfall.

The global mean values for the cloud liquid water fields shown in Plate 2 are 0.081 and 0.075 kg m^{-2} for August 1987 and February 1988, respectively. The results of Njoku and Swanson have a slightly lower global mean of 0.07 kg m^{-2}, which is undoubtedly caused by the lower liquid water values in the tropics. The total global cloud liquid water mass in the marine environment is determined to be about 2.4×10^{13} kg for both months. This is in contrast to a value of 8.7×10^{13} kg found by *Akvilonova et al.* [1973] averaged over 5 days from September 23 to 27, 1968. The factor of 3–4 difference between these estimates is most likely related to the retrieval of cloud liquid water in areas of precipitation or possible biases.

As an independent verification of the monthly mean global distributions of cloud liquid water, a comparison is made to the total cloudiness compiled by ISCCP [*Schiffer and Rossow*, 1983], which are satellite-derived products provided on a $2.5°\times2.5°$ global grid. Figure 13 shows latitudinal profiles of SSM/I cloud liquid water and total cloud amount over the oceans for August 1987 and February 1988. There is excellent agreement in the summer hemisphere for both months where the clouds are composed primarily of water. For the winter hemisphere the correspondence deteriorates because a large number of the clouds are composed of ice, which are mostly transparent to microwaves at 19.35 and 37 GHz.

7. CONCLUSIONS

A method of simultaneously retrieving both integrated cloud liquid water and water vapor over the oceans using satellite-based passive microwave radiometry is presented. The technique consists of a simple physical model, which in part derives from the physical PWC scheme of *Tjemkes et al.* [1991] and exploits measurements at 19.35 and 37 GHz from the SSM/I. Since the method is generally robust and can be used over most areas of the oceans, it may prove useful for global studies of the atmospheric hydrological cycle.

The results of a preliminary verification of cloud liquid water determined from satellites have shown the retrievals to be consistent with coincident estimates of liquid water from independent ground-based measurements in the subtropics and middle to high latitudes with rms differences ranging from 0.04 to 0.05 kg m^{-2}, with the most accurate retrievals

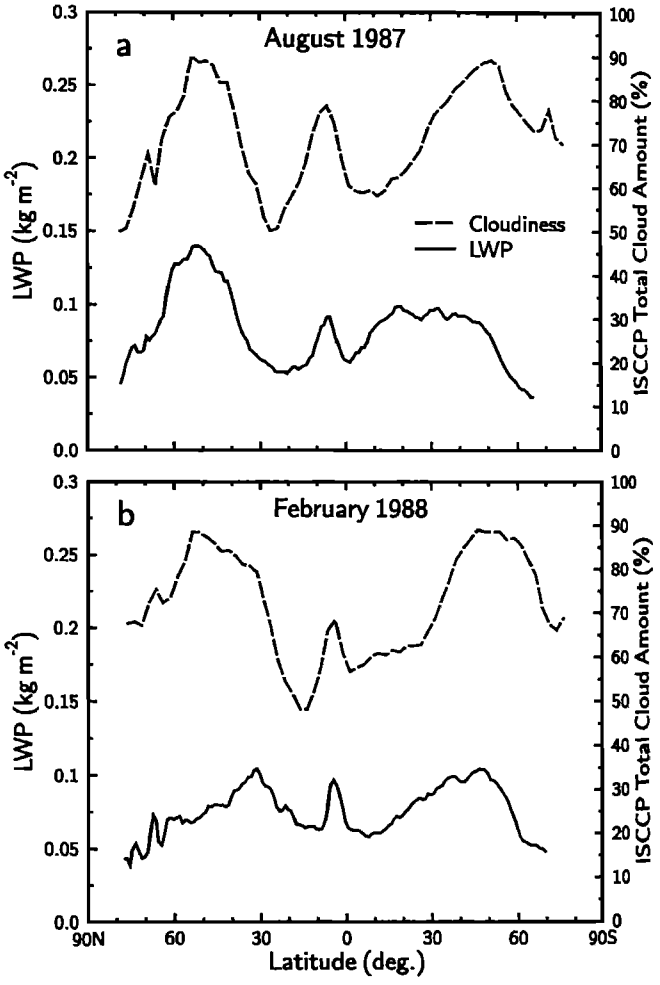

Fig. 13. Zonal distributions of cloud liquid water (kg m^{-2}) and International Satellite Cloud Climatology Project (ISCCP) total cloudiness over the oceans for (*a*) August 1987 and (*b*) February 1988.

occurring in areas of marine stratocumulus clouds. The comparisons at the tropical sites were generally disappointing, which was mainly a result of the difficulty in estimating liquid water from either satellite or ground-based systems in the tropical Pacific. A comparison to near-coincident LWP inferred from visible reflectances for California marine stratus clouds shows consistent agreement. Further comparisons in specific regions and under limited conditions to other SSM/I liquid water algorithms yielded mixed results, with generally good agreement for the *Petty* [1990] and *Hargens* [1992] algorithms (rms differences of 0.03 and 0.02 kg m^{-2}, respectively) but large discrepancies for the *Alishouse et al.* [1990] method (rms differences of 0.07 kg m^{-2}). Also, a qualitative comparison of the SSM/I-derived LWP field to near-coincident visible satellite imagery in the West Pacific showed very good correspondence.

For nonprecipitating clouds it was shown from a simple error analysis that the degree of confidence in the retrieved liquid water depends on the type of atmospheric and surface conditions and on the amount of liquid water. The relative errors are anticipated to range from about 25% to 40%, but occasionally reach 50%, with the largest errors occurring in environments with an abundance of water vapor and for low cloud liquid water. Retrievals for a limited number of SSM/I observations in known clear sky regions resulted in a standard deviation of 0.016 kg m^{-2}, which provided an estimate of the minimum retrieval uncertainties. Errors in the retrieval associated with differences in the footprint sizes of the 19.35- and 37-GHz channels are shown to be smaller than errors caused by imprecise knowledge of the state of the atmosphere and sea surface.

The global fields of cloud liquid water derived from the present method appear to give reasonable patterns that correspond to well-known features of the global circulation. A comparison to SMMR-derived cloud liquid water reveals a close correspondence at high latitudes and slightly less agreement in terms of magnitude at lower latitudes. The global mean cloud liquid water over the oceans is found to be greater for the northern hemisphere summer (0.081 kg m^{-2}) than for the winter (0.075 kg m^{-2}). Other comparisons to independent measurements of total cloudiness on a monthly mean basis show good agreement except in the winter hemisphere where ice clouds are prevalent.

Several ways are proposed to refine the model developed in this study. Specifically, one might add other types of ancillary information, such as IR data, to improve estimates of the effective cloud temperature. Information about the vertical temperature structure of the atmosphere based on SSM/T (special sensor microwave/temperature) sounder retrievals might be incorporated into the model. Retrievals of SST and better estimates of surface winds using lower frequency channels of future instruments, such as the high resolution microwave spectrometer sounder (HIMSS) proposed for the Earth Observing System (EOS) satellites and the Tropical Rainfall Measuring Mission (TRMM) microwave imager can also help to improve the model. A further advancement in the retrieval of PWC in a dry atmosphere may be achieved by including the 22.235-GHz channel, which is far more sensitive to changes in smaller water vapor amounts than the 19.35 GHz channels.

This study has demonstrated that adequate estimates of integrated cloud liquid water can be obtained from SSM/I measurements over the oceans and outside regions of precipitation, with slightly less accurate retrievals in the tropics. Further research efforts are needed to monitor oceanic cloud liquid water over long periods of time at various sites, especially in the tropics, to provide reliable "ground truth" data sets to validate methods such as described in this paper. These ground-based and satellite data sets will be valuable tools for testing those general circulation models that currently predict cloud liquid water [e.g., *Heise and Roeckner*, 1990; *Smith*, 1990] and will play a vital role in better understanding the significance of clouds in climate and climate change.

Acknowledgments. Thanks go out to NESDIS (National Environmental Satellite, Data, and Information Center) for supplying the SSM/I antenna temperature tapes. We are indebted to Jack Snider for the San Nicolas Island ground-based cloud liquid water data, C. Prabhakara for the SMMR LWP data, John Alishouse for the Kwajalein Island liquid water data. Ute Hargens for the North Sea radiosonde and liquid water observations, and Y. Han for the Saipan Island liquid water and ceilometer data. Sincere thanks go to Grant Petty for providing his valuable cloud-free data set and to Chris Kummerow for the SSM/I resolution enhancement coefficients. We are also grateful to Andy Jones for the satellite data fusion and remapping software package called PORTAL. The AVHRR data were kindly supplied by the Satellite Data Services Division of NOAA. The supercomputer facilities at NCAR provided the major computing support. This research was funded by a NASA Global Change Fellowship and, in part, by NOAA grants NA90AA-D-AC822 and NA90RA00077 and NASA grant NAG5-1592.

REFERENCES

Adler, R. F., R. A. Mack, N. Prasad, H.-Y. M. Yeh, and I. M. Hakkarinen, Aircraft microwave observations and simulations of deep convection from 18 to 183 GHz. Part I: Observations, *J. Atmos. Oceanic Technol.*, *7*, 377-391, 1990.

Akvilonova, A. B., A. Y. Basharinov, A. K. Gorodetskiy, A. S. Gurvich, M. S. Krylova, B. G. Kutuza, D. T. Matveyev, and A. P. Orlov, Cloud parameters measured from the Cosmos-384 satellite, *Atmos. Oceanic Phys.*, *9*, 187-189, 1973.

Akvilonova A. B., and B. G. Kutuza, Microwave radiation of clouds, *Radio Eng. Electron. Phys.*, *24*, 12-24, 1979.

Albrecht, B. A., C. W. Fairall, D. W. Thomson, A. B. White, J. B. Snider, and W. H. Schubert, Surface-based remote sensing of the observed and the adiabatic liquid water content of stratocumulus clouds, *Geophys. Res. Lett.*, *17*, 89-92, 1990.

Alishouse, J. C., J. B. Snider, E. R. Westwater, C. T. Swift, C. S. Ruf, S. A. Snyder, J. Vongsathorn, and R. R. Ferraro, Determination of cloud liquid water content using the SSM/I, *IEEE Trans. Geosci. Remote Sens.*, *28*, 817-822, 1990.

Basharinov, A. Y., A. S. Gurvich, and S. T. Yegorov, Determination of geophysical parameters from data on thermally-induced radioemission obtained with the Cosmos 243 satellite, *Dokl. Akad. Nauk SSSR*, *188*, 1273-1276, 1969.

Bates, J. J., High-frequency variability of Special Sensor Microwave/Imager derived wind speed and moisture during an intraseasonal oscillation, *J. Geophys. Res.*, *96*, 3411-3423, 1991.

Chang, A. T. C., and T. T. Wilheit, Remote sensing of atmospheric water vapor, liquid water, and wind speed at the ocean surface by passive microwave techniques from the Nimbus 5 satellite, *Radio Sci.*, *14*, 793-802, 1979.

Curry, J. A., C. D. Ardeel, and L. Tian, Liquid water content and precipitation characteristics of stratiform clouds as inferred from satellite microwave measurements, *J. Geophys. Res.*, *95*, 16,659-16,671, 1990.

Gagarin, S. P., and B. G. Kutuza, Influence of sea surface roughness and atmospheric inhomogeneities on microwave radiation of the atmosphere-ocean system, *IEEE J. Ocean. Eng.*, *OE-8*, *2*, 62-70, 1983.

Goodberlet, M. A., C. T. Swift, and J. C. Wilkerson, Remote

sensing of ocean surface winds with the Special Sensor Microwave/Imager, *J. Geophys. Res.*, *94*, 14,547-14,555, 1989.

Grody, N. C., A. Gruber, and W. C. Shen, Atmospheric water content over the tropical Pacific derived from the Nimbus-6 scanning microwave spectrometer, *J. Appl. Meteorol.*, *19*, 986-996, 1980.

Grody, N. C., Remote sensing of atmospheric water content from satellites using microwave radiometry, *IEEE Trans. Antennas Propag.*, *AP-24*, 155-162, 1976.

Han, Y., and D. W. Thomson, Determination of integrated water vapor and liquid water by a combination of a microwave radiometer and a ceilometer during TCM-90 Experiment, paper presented at the Third Specialists Meeting on Microwave Radiometry and Remote Sensing Applications, pp. 363-367, NOAA Environ. Res. Lab., Boulder, Colorado, 1992.

Hargens, U., Remote sensing of cloud liquid water during ICE'89, paper presented at the Third Specialists Meeting on Microwave Radiometry and Remote Sensing Applications, pp. 27-31, NOAA Environ. Res. Lab., Boulder, Colorado, 1992.

Heise E., and E. Roeckner, The performance of physically based cloud schemes in general circulation models, *Beitr. Phys. Atmos.*, *63*, 1-13, 1990.

Hill, G., Comparison of simultaneous airborne and radiometric measurements of supercooled liquid water, *J. Appl. Meteorol.*, *30*, 1043-1046, 1991.

Hill, G., Further comparisons of simultaneous airborne and radiometric measurements of supercooled liquid water, *J. Appl. Meteorol.*, *31*, 397-401, 1992.

Hogg, D. C., F. O. Guiraud, J. B. Snider, M. T. Decker, and E. R. Westwater, A steerable dual-channel microwave radiometer for measurement of water vapor and liquid in the troposphere, *J. Clim. Appl. Meteorol.*, *22*, 789-806, 1983.

Jones, A. S., and T. H. Vonder Haar, Passive microwave remote sensing of cloud liquid water over land regions, *J. Geophys. Res.*, *95*, 16,673-16,683, 1990.

Katsaros, K. B., and R. M. Lewis, Mesoscale and synoptic scale features of North Pacific weather systems observed with the Scanning Multichannel Microwave Radiometer on Nimbus 7, *J. Geophys. Res.*, *91*, 2321-2330, 1986.

Liebe, H. J., An updated model for millimeter wave propagation in moist air, *Radio Sci.*, *20*, 1069-1089, 1985.

Liu, G., and J. A. Curry, Retrieval of precipitation from satellite microwave measurement using both emission and scattering, *J. Geophys. Res.*, *97*, 9959-9974, 1992.

Liu, W. T., W. Tang, and F. J. Wentz, Precipitable water and surface humidity over global oceans from Special Sensor Microwave Imager and European Center for Medium Range Weather Forecasts, *J. Geophys. Res.*, *97*, 2251-2264, 1992.

Njoku, E. G., and L. Swanson, Global measurements of sea surface temperature, wind speed, and atmospheric water content from satellite microwave radiometry, *Mon. Weather Rev.*, *111*, 1977-1987, 1983.

Paltridge, G. W., Cloud-radiation feedback to climate, *Q. J. R. Meteorol. Soc.*, *106*, 895-899, 1980.

Pandey, P. C., E. G. Njoku, and J. W. Waters, Inference of cloud temperature and thickness by microwave radiometry from space, *J. Clim. Appl. Meteorol.*, *22*, 1894-1898, 1983.

Petty, G. W., On the response of the Special Sensor Microwave/Imager to the marine environment – Implications for atmospheric parameter retrievals, Ph.D. dissertation, 291 pp., Univ. of Washington, Seattle, 1990.

Petty, G. W., and K. B. Katsaros, The response of the SSM/I to the marine environment. Part I: An analytic model for the atmospheric component of observed brightness temperatures, *J. Atmos. Ocean. Technol.*, *9*, 746-761, 1992*a*.

Petty, G. W., and K. B. Katsaros, Nimbus 7 SMMR precipitation observations calibrated against surface radar during TAMEX, *J. Appl. Meteorol.*, *31*, 489-505, 1992*b*.

Prabhakara, C., I. Wang, A. T. C. Chang, and P. Gloerson, A statistical examination of Nimbus-7 SMMR data and remote sensing of sea surface temperature, liquid water content in the atmosphere and surface wind speed, *J. Clim. Appl. Meteorol.*, *22*, 2023-2037, 1983.

Prabhakara, C., D. A. Short, W. Wiscombe, and R. S. Fraser, Rainfall over oceans inferred from Nimbus 7 SMMR: Application to 1982-83 El Niño, *J. Clim. Appl. Meteorol.*, *25*, 1464-1474, 1986.

Reynolds, R. W., A real–time global sea surface temperature analysis, *J. Clim.*, *1*, 75-86, 1988.

Robinson, W. D., C. Kummerow, and W. S. Olson, A technique for enhancing and matching the resolution of microwave measurements from the SSM/I instrument, *IEEE Trans. Geosci. Remote Sens.*, *30*, 419-429, 1992.

Rosenkranz, P. W., D. H. Staelin, and N. C. Grody, Typhoon June (1975) viewed by a scanning microwave spectrometer, *J. Geophys. Res.*, *83*, 1857-1868, 1978.

Schiffer, R. A., and W. B. Rossow, The International Satellite Cloud Climatology Project (ISCCP): The first project of the World Climate Research Programme, *Bull. Am. Meteorol. Soc.*, *64*, 779-784, 1983.

Schluessel, P., and W. J. Emery, Atmospheric wator vapour over oceans from SSM/I measurements, *Int. J. Remote Sens.*, *11*, 753-766, 1990.

Schubert, W. H., S. K. Cox, P. E. Ciesielski, and C. M. Johnson-Pasqua, Operation of a ceilometer during the FIRE marine stratocumulus experiment, *Pap. 420*, 28 pp., Colo. State Univ., Dep. of Atmos. Sci., Fort Collins, 1987.

Smith, R. N. B., A scheme for predicting layer clouds and their water content in a general circulation model, *Q. J. R. Meteorol. Soc.*, *116*, 435-460, 1990.

Somerville, R. C. J., and L. A. Remer, Cloud optical thickness feedbacks in the CO_2 climate problem, *J. Geophys. Res.*, *89*, 9668-9672, 1984.

Spencer R. W., H. M. Goodman, R. E. Hood, Precipitation retrieval over land and ocean with the SSM/I: Identification and characteristics of the scattering signal, *J. Atmos. and Oceanic Technol.*, *6*, 254-273, 1989.

Stephens, G. L., Radiation profiles in extended water clouds, II: Parameterization schemes, *J. Atmos. Sci.*, *35*, 2123-2132, 1978.

Stephens, G. L., and T. J. Greenwald, The Earth's radiation budget and its relation to atmospheric hydrology, 2, Observations of cloud effects, *J. Geophys. Res.*, *96*, 15,325-15,340, 1991.

Tjemkes, S. A., G. L. Stephens, and D. L. Jackson, Spaceborne observation of columnar water vapor: SSMI observations and algorithm, *J. Geophys. Res.*, *96*, 10,941-10,954, 1991.

Westwater, E. R., The accuracy of water vapor and cloud liquid determination by dual-frequency ground-based microwave radiometry, *Radio Sci.*, *13*, 677-685, 1978.

Wilheit, T. T., A model of the microwave emissivity of the ocean's surface as a function of wind speed, *IEEE Trans. Geosci. Electron.*, *GE-17*, 244-249, 1979.

Wilheit, T. T., and A. T. C. Chang, An algorithm for retrieval of ocean surface and atmospheric parameters from the observations of the Scanning Multichannel Microwave Radiometer, *Radio Sci.*, *15*, 525-544, 1980.

T. J. Greenwald, D. L. Jackson, G. L. Stephens, and T. H. Vonder Haar, Department of Atmospheric Science, Colorado State University, Fort Collins, CO 80523.

(Received June 21, 1992;
revised February 1, 1993;
accepted February 5, 1993.)